Collision Avoidance Algorithm for Unmanned Surface Vehicle Based on Improved Artificial Potential Field and Ant Colony Optimization

Wen Ou[1, a], Xuan Guo[2, b *]

[1]Key Laboratory of Image Information Processing and Intelligent Control of Education Ministry of China School of Automation Huazhong University of Science and Technology, Wuhan, China;

[2]School of Automation Wuhan University of Technology Wuhan, China;

[a]owen@hust.edu.cn, [b]luluche123@sina.com

Abstract. There is a growing concern to design collision avoidance algorithm for unmanned surface vehicle (USV) as a solution to many naval and civilian requirements. Due to the anti-jamming performance of the traditional collision avoidance algorithm decrease with the influence of environmental disturbances, resulting in the problems of frequent steering and overshoot when USV is sailing under harsh sea condition. An improved collision avoidance algorithm based on improved artificial potential field and ant colony optimization is proposed in this paper. And, a power function based on the change of the distance to the obstacle is proposed. This improved combination is to solve the problem of frequent steering and overshoot of USV's control system with good robustness during collision avoidance. The results of simulation and experiment demonstrate the proposed method is more efficient and more capable to avoid the obstacles through route planning particularly in the presence of large disturbances.

Keywords: Unmanned surface vehicle, collision avoidance, route planning, artificial potential field algorithm, ant colony algorithm.

1. Introduction

The unmanned surface vehicle (USV) is an unmanned ship. Mainly used to perform dangerous missions and tasks that are not suitable for manned vessels. In recent years, USV has been widely used to conduct scientific research in the fields of Oceanography [1], meteorology [2], military and commercial applications [3]. USV can navigate safely under the actual marine environment and complete various tasks including anti-submarine warfare and minesweeping, patrol and interdiction [4,6]. Compared to the traditional manned vehicle [35], USV has a lot of outstanding tactical and technical characteristics, for instance, small volume, invisibility, no dangerous about casualties and so on [7,8]. When the USV encounters an obstacle and ship, it is necessarily to avoid obstacles autonomously. Artificial potential field algorithm is a relatively common method of local route planning and is often applied to collision avoidance [33,34].

Nowadays, many intelligent collision avoidance methods for USV have been proposed [31,32]. A method that increase the virtual target point was proposed. In order to solve the problem that the artificial potential field method could easily fall into the local minimum point [9]; A power function based on the target distance was proposed that improve the repulsive field function. In order to solve the problem of unreachable goals [10]; A method that inserting relative velocity field potentials and intermediate targets was proposed. In order to improve the situation that it's easily trapped in local minima [11]; The repulsive force function based on a modified Gaussian function and the method of repulsive component modification are proposed that solve the problem of local minimum [12]; A fuzzy potential field based on the change of target distance was proposed that improve the repulsive field function [13]; A method of global optimization of parameters based on quantum particle swarm for collision avoidance of dynamic targets was proposed [14]; An escape function based on the target distance was proposed that improve the repulsive field function and used to jump out of the local minimum [15]. Although the above methods solve the problem of traditional artificial potential field algorithm. However, it is applied to USV without considering the constraints of its maneuverability

model. Therefore, the above methods are not better satisfied with USV's maneuverability requirements.

In this work, an improved collision avoidance algorithm based on improved artificial potential field algorithm and ant colony optimization is to solve the problem of frequent steering of USV in harsh sea condition. Due to the traditional potential field intensity changes frequently, a power function based on the change of the distance to the obstacle is to improve the problem that the planned track curve is oscillated. The constraint conditions of USV's collision avoidance are established in the algorithm, so that, the planned track curve is satisfied with the requirements of motion control maneuverability. And, the collision avoidance evaluation model is established that to calculate the evaluation value of each planned track curve. Then, the optimal route is searched by the ant colony algorithm based on the evaluation value. Finally, the results of simulation and real ship experiment demonstrate the effectiveness of this method. This combination of the algorithm has good robustness.

The rest of the paper are organized as follows: Section 2 presents the problems of USV during collision avoidance, and studied model of USV in this work. Section 3 describes an improved collision avoidance algorithm based on artificial potential field and ant colony optimization. Section 4 provides simulation results and experimental results. Section 5 gives the conclusion of the work.

2. Problem Formulation

The research of the collision avoidance algorithm is developed on the mobile robots. However, when this method is applied to the USV, the problem of maneuverability of the USV must be considered. The changes of relative distance from the obstacle due to the changes of USV's position at each moment. This results in a significant change in the strength of the potential field, that is, the intensity of the potential field changes frequently. When USV is sailing under harsh sea conditions, the change frequency of USV's heading due to the change frequency of the potential field, resulting in the problems of frequent steering and overshoot.

Due to the changes of relative distance between the obstacle and USV's position at each moment, this results in a significant change frequently in the intensity of the potential field. When USV encountered an obstacle in an emergency, due to the reason why the potential field change frequently, resulting in the problem that USV's heading change frequently. Furthermore, the anti-jamming performance of the traditional artificial potential field algorithm decrease with the influence of environmental disturbances, resulting in the problems of frequent steering and overshoot under harsh sea conditions or high-risk environments. Compared to the traditional mobile robot, it can steer with two-wheeled differential or stop with decelerating, so that, it can turn a large angle along the planned route. However, USV cannot steer at a large angle along the planned route through steering control. Due to the traditional artificial potential field method is not better satisfied with USV's maneuverability requirements. Therefore, an intelligent collision avoidance algorithm for USV is necessarily proposed that solve this problem.

It is difficult to meet the requirements of USV’s maneuverability for the collision avoidance route planned for the traditional artificial potential field method. The constraint condition of collision avoidance and the avoidance evaluation model of USV are established necessarily in the algorithm. Then, the evaluation value of the route planning is calculated by the evaluation model. USV used in the work is shown in Fig 1, with the main parameters shown in Table 1.

Fig. 1 Images of the USV

Table 1 Main parameters of unmanned surface vehicle

Parameter	Value
Length /m	8.075
Vertical length /m	8
Draft depth /m	0.6
Molded depth/m	1.15
Full loaded displacement/T	3.2
Maximum speed /kn	12
Cruising speed /kn	6
Propulsion mode	water jet propulsion

Because of the interference of wind, waves and currents, the maneuvering motion model [16] of USV is expressed as:

$$\begin{cases} T_1T_2\ddot{\Psi}+(T_1+T_2)\dot{\Psi}+\Psi+a\Psi^3=K\delta+KT_3\dot{\delta}+f_a+f_w+f_l \\ T_1T_2=(m+\lambda_{22})(I_z+\lambda_{66})/C \\ T=T_1+T_2-T_3 \end{cases} \tag{1}$$

where Ψ is the course angle, δ is the rudder angle, T is the rudder index, K is the rotational index, the other parameters is the USV maneuverability parameters. f_a is equivalent disturbance rudder angle of the wind, f_w is equivalent disturbance rudder angle of the disturbances due to waves, f_l is equivalent disturbance rudder angle of the disturbances due to currents.

3. Design of Collision Avoidance Algorithm for USV

In this work, an intelligent collision avoidance algorithm based on improved artificial potential field and ant colony optimization is designed. And, a power function based on the change of the distance from the target point is proposed. In order to realize the function of local route planning and collision avoidance of USV in the complex marine environment such as harsh sea conditions and narrow waters. The factors of relative position for target point and USV are added to the potential field function that solve the problem that target point is unreachable. And the problem of a local minimum point is solved by a method of dynamically adjusting the repulsive force field. The block diagram of the USV's collision avoidance algorithm is shown in Fig. 2.

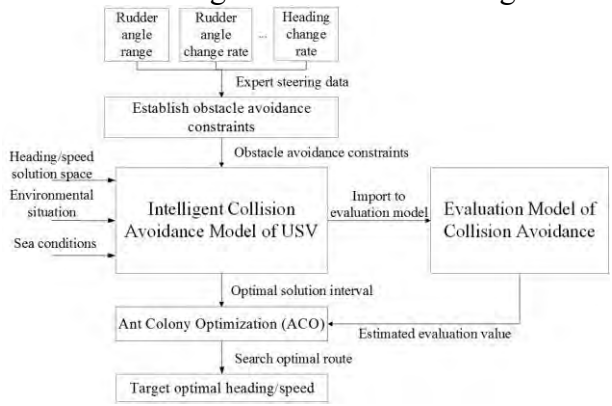

Fig. 2 Block diagram of USV's collision avoidance algorithm

Furthermore, constraint conditions based on the steering range, the change rate of rudder angle, the change rate of heading, the steering data of expert are established. And, the collision avoidance model base on the collision risk is established. At the same time, an evaluation model related to autonomous collision avoidance performance indicators is established, such as sailing time, steering frequency, the shortest distance from obstacles, the shortest distance from the target point, and average corner of the entire route. Finally, the optimal target heading and speed are searched by the heuristic ant colony algorithm.

3.1 Improvement of Artificial Potential Field.

Usually, USV sails toward the target point under the gravitational force of the artificial potential field. When USV is closer to the target point, the attraction force is smaller. And when USV approaches the target point indefinitely, the attraction force tends to zero. The general form of gravitational potential field function is as follows:

$$U_g(q) = \frac{1}{2}\xi(q_{goal} - q)^2 \tag{2}$$

where U_g is the gravitational potential field function of target point which USV is subjected at a certain point; ξ is the gain factor of the gravitational potential field; q is the current position of USV; And q_{goal} is the position of the target point. The negative gradient of distance is calculated by gravitational potential field function. And the gravitational function expression can be expressed as:

$$F_g(q) = -\nabla U_g(q) = \xi(q_{goal} - q) \tag{1}$$

The repulsive force function of most artificial potential fields is calculated based on the relative distance from obstacles. The change of relative distance from obstacles, due to the change of USV's position at each moment, resulting in the change of potential field frequently. This situation causes the change of heading frequently and frequent steering. Based on the description of the ship's maneuverability principle [18], frequent steering should be avoided during the navigation of USV. Furthermore, route planning can also be affected by frequent steering. Therefore, a power function based on the change of the distance to the obstacle is designed to solve the problem of frequent steering. Its expression is as follows:

$$U_r(q) = \begin{cases} \eta \dfrac{(\rho_{\max} - (q - q_o))^n}{\rho_{\max} - \rho_{\min}} \times (\dfrac{1}{6})^{n-1} & (q - q_0) \le \rho \\ 0 & (q - q_0) > \rho \end{cases} \tag{2}$$

where U_r is the repulsive potential field function of obstacle that USV is subjected at a certain point; η is the gain factor of repulsive potential field; q is the current position of USV; q_o is the position of obstacle; $\rho_{\max}$ is the maximum influence radius of obstacle; $\rho_{\min}$ is the impact radius of obstacle; ρ is the influence of obstacle radius. n is the control parameter of potential field function. When n is larger, the potential field function converges faster. When n is smaller, the path oscillates more violently.

The factor of a relative position of the target point and USV is established. And the repulsive field function is multiplied by this formula to solve the problem that traditional artificial potential field method is unreachable. When the obstacle is close to a target point, the repulsive force field is also affected by the gravitational field. When the USV is near the target point, its repulsive force approaches zero. The further improved repulsive potential field function is as follow:

$$U_r(q) = \begin{cases} \eta(q_{goal} - q)^n \times \dfrac{(\rho_{\max} - (q - q_o))^n}{\rho_{\max} - \rho_{\min}} \times (\dfrac{1}{6})^{n-1} & (q - q_0) \le \rho \\ 0 & (q - q_0) > \rho \end{cases} \tag{3}$$

where q is the current position of USV; q_{goal} is the position of the target point; $(q_{goal} - q)$ is the distance between USV and the point. The repulsion received by USV is a negative gradient of the potential field. The expression is as follow:

$$F_r(q) = \begin{cases} (\dfrac{1}{6})^{n-1} n\eta(q_g - q)^{n-1} D(q) \dfrac{(\rho_{\max} - (q - q_o))^{n-1}}{\rho_{\max} - \rho_{\min}} & (q - q_0) \le \rho \\ 0 & (q - q_0) > \rho \end{cases} \tag{4}$$

where $D(q) = (\rho_{\max} - 2q + q_o + q_g)$. Furthermore, USV moves forward under the gravitational force of target point and is also affected by the repulsive force of obstacles. The direction of the repulsion is opposite to obstacle. Under the combined force of gravitational force and repulsive force, the force of artificial potential field is shown in Fig. 3.

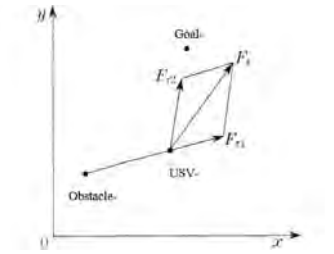

Fig. 3 The force of USV in the artificial potential field

3.2 Model of Collision Risk.

Due to the different problems of collision avoidance scenarios between dynamic vessels and static obstacles, the collision avoidance algorithm of this paper is modified. According to the "International Regulations for Preventing Collisions at Sea" in the literature [30], a collision avoidance model based on the encounter rules of vessels was established. And, a collision risk model based on minimum meeting time ($Tcpa$) and minimum meeting distance ($Dcpa$) is established. The fuzzy membership function is established respectively by $Dcpa$ and $Tcpa$, which is divided into space and time collision risk function (SR,TR). Finally, the collision risk is calculated by the synthetic factors. The spatial collision risk model established is as follows:

$$u(SR)=\begin{cases} 1 & Dcpa \le dcpa_{d\min} \\ \dfrac{1}{\rho}\left[1-\sin\left(\dfrac{\pi(Dcpa-\frac{dcpa_{d\min}+d_{\max}}{2})}{d_{\max}-dcpa_{d\min}}\right)\right] & dcpa_{d\min} \le Dcpa \le d_{\max} \\ 0 & Dcpa \ge d_{\max} \end{cases} \tag{7}$$

where $u(SR)$ is the membership function of $Dcpa$; $dcpa_{d\min}$ is the safe passing distance; $d_{\max}$ is the closest encounter distance of the two ships at the latest steering point, $dcpa_{d\min}=L_0/2+L_1/2$; L_0 is the length of the ship; L_1 is the length of the target ship; $d_{\min}$ is the distance between the two ships at the latest steering point. $\rho=2$ is the control parameter of the space collision risk function. The time collision risk model established in this work is as follows:

$$u(TR)=\begin{cases} 1 & Tcpa \le t_{\min} \\ \left(\dfrac{t_{\max}-Tcpa}{t_{\max}-t_{\min}}\right)^2 & t_{\min} \le Tcpa \le t_{\max} \\ 0 & Tcpa \ge t_{\max} \end{cases} \tag{8}$$

where $u(TR)$ is the membership function value of $Tcpa$; d_{Arena} is the boundary value of the dynamic distance; $t_{\max}, t_{\min}$ is the two boundary values of the $Tcpa$ membership function; $t_{\min}$ is the $Tcpa$ value when the ship reaches the latest steering point; $t_{\max}$ is the $Tcpa$ value when the distance between the two ships is the boundary value. These two values are difficult to implement in the program. Considering the safety of their collision avoidance, $t_{\min}=d_{\min}/v_r$, $t_{\min}=d_{Arena}/v_r$. Both of these values are larger than the corresponding value of $Tcpa$. In some cases, the time for collision avoidance is advanced. Base on classifying the encounters of dynamic vessels, the collision risk is calculated by the encounter information of the obstacles. Combined with the risk of space and time collision, the established collision risk model is as follows:

$$CRI=u(SR)\oplus u(TR)=\min\left\{\frac{[\alpha\times u(SR)]^2+[\beta\times u(TR)]^2}{2\alpha\beta},1\right\} \tag{9}$$

where CRI is the value of the ship's collision risk. Furthermore, the situation of each obstacle is judged by this collision avoidance model. The situation is mainly divided into in front encounter mode, cross encounter mode and chase mode. Due to the maneuverability of obstacles in different orientations, the situation of the USV and obstacles is divided into seven categories. The situation is divided into encounter in front, small angle crossing on the right, large angle crossing on the right, USV chasing obstacle, obstacle chasing USV, large angle crossing on the left and small angle

crossing on the left. The encounter situation between the USV and the dynamic vessel in this work is shown in Fig. 4.

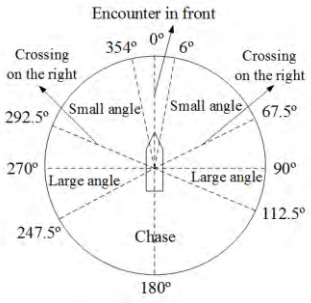

Fig. 4 The meeting situation diagram of USV and dynamic vessels

3.3 Constraint Model of Collision Avoidance.

The collision avoidance constraint conditions of USV's motion model is necessarily established, due to the planning route of traditional artificial potential field algorithm does not meet maneuverability requirements. The range of steering, the rate of change of rudder angle, and the rate of heading change are taken as the constraints of USV's motion model. If the planned route satisfies the constraint condition, the next calculation is performed. Otherwise, the planned route at a previous time is maintained. To avoid damage of the rudder due to the excessive rotation range of the rudder angle. The steering range of USV is limited as follows:

$$\delta(\theta) = \begin{cases} \delta_{\min} & \theta \le \theta_{\min} \\ \delta_{\max} & \theta \ge \theta_{\max} \end{cases} \tag{5}$$

where $\delta(\theta)$ is the rudder angle output; $\delta_{\min}$ is the maximum limit amplitude of left rudder, $\delta_{\max}$ is the maximum rudder angle limit of right rudder, $\theta_{\min}$ is the value of -35°, and $\theta_{\max}$ is the value of 35°.

According to the literature's [18] description, when USV's speed increases, too large rudder angle cause two problems. First, excessive rudder angle requires the steering gear which has a large driving power and sufficient mechanical strength; Second, when the speed increases, an excessive rudder angle cause the rudder's lift to drop, and the surface of the rudder produces a hollow bubble. And, the manipulation of USV is directly affected by its speed. Therefore, when the USV's speed increases, the range of rudder angle limit should be reduced. The right rudder angle limit range can be determined by the following formula:

$$\delta_{\max} = \frac{2r_{\max}L}{Kv} \tag{6}$$

where L is the length of USV; v is the speed of USV, K is the rotation parameter, $r_{\max}$ is the maximum steering angular velocity of USV; Similarly, $\delta_{\min}$ can also be derived from the above formula.

The functional relationship between rudder angle and heading angle is established by the $K-T$ maneuverability equation of USV. That is, the change of rudder angle at each moment corresponds to the change of heading angle. If the heading value at next moment does not satisfy above constraints, the heading value at previous moment is maintained, or the maximum limited heading angle is maintained. According to the maneuverability parameters of USV [19], the overall transfer function expression of ship can be derived. The expression of time relationship between USV's heading angle and rudder angle is as follow:

$$G(s) = \frac{K}{Ts^2 + s} = \frac{\varphi}{\delta} \tag{7}$$

Where K is the rotation parameter; T is the stability parameter, that is, the maneuverability parameter of USV, which can be calculated by the Z-type test; φ is the heading angle of USV; δ is the rudder angle of USV; s denotes a derivative relation in a time state, for example: $r = \varphi \cdot s$. Through the above formula and the K and T parameters, the range of USV's heading change rate is calculated as follows:

$$\Delta\varphi(\theta)=\begin{cases}\dfrac{K\delta_{\min}}{Ts^2+s}=-1.0472 & \theta\le\theta_{\min}\\ \dfrac{K\delta_{\max}}{Ts^2+s}=1.0472 & \theta\ge\theta_{\max}\end{cases} \tag{8}$$

where $\Delta\varphi(\theta)$ is the range of USV's heading change rate. Furthermore, the maneuverability of USV is limited by the change rate of steering speed, that is, the rudder angle acceleration. However, the USV's steering mode is uniform speed steering, that is, rudder angle acceleration is zero. Therefore, this factor is not considered as a constraint. In collision avoidance simulation, USV cannot be treated as a particle. It is also necessary to take into account its model, including the model of steering engine and the model of motion.

3.4 Evaluation Model.

An evaluation model of collision avoidance performance index is established to provide an evaluation value for planning route. The criteria for collision avoidance performance evaluated by references [20] as follows: sailing time, steering frequency, the minimum distance from obstacles, the minimum distance from end points, and average corner of entire path (path smoothness) etc. The optimality of route and the safety of path are considered by the evaluation method and can be applied in the evaluation model of collision avoidance [25,26]. The evaluation function is divided into two parts: whether the collision avoidance is qualified and the performance of the algorithm under a qualified condition. The unqualified performance indicators for collision avoidance are as follows:

1) USV collided with an obstacle;
2) The minimum distance between USV and obstacle $D_{\min} < D_{safe}$, that is the minimum safety distance. It's set at 1.5 times length of the ship; Therefore, D_{safe} is about 10 m;
3) Sailing time $T > 20\min$, the time required for USV to sail along a semicircle with a diameter;

In the collision avoidance test of USV, if any one of the above conditions is satisfied, it means the test failed.

The five indicators of sailing time T, steering frequency f_{angle}, the shortest distance from the obstacle $D_{\min}$,the shortest distance from the target point D_{goal}, and average corner θ_{av} of the entire route are normalized. Then, T^*, f^*_{angle}, $D^*_{\min}$, D^*_{goal}, θ^*_{av} can be derived, and the weighted sum of normalized values is calculated by this method. Therefore, the evaluation value of USV's collision avoidance can be evaluated as follows:

$$P=k_1(1-T^*)+k_2(1-f_{angle})+k_3D^*_{\min}+k_4(1-D^*_{goal})+k_5(1-\theta^*_{av}) \tag{9}$$

where $k_i(i=1,2,3,4,5)$ is the weight coefficient of each indicator. The value of P is directly proportional to the quality of USV's collision avoidance. The weights of the evaluation coefficients are shown in Table 2.

Table 2 Evaluation index weight coefficient distibution

Index	Weights
Sailing time	0.15
Steering frequency	0.2
The shortest distance from obstacles	0.3
The shortest distance from the target point	0.15
Average steering angle	0.2

3.5 Ant Colony Algorithm.

Ant colony algorithm (ACO) is based on the probability-type bionic evolutionary intelligence algorithm. The basic mathematical model of ant colony algorithm can be applied to the route planning problem of USV and can be used to solve the problem of path optimization in location traversal [21,22]. It is necessary to traverse all locations exactly and find the shortest path from the beginning to the end. Compared with other heuristic algorithms, ant colony algorithm has good robustness and the ability in search performance, and it is easy to implement in parallel [24]. Ant colony algorithm model is slightly modified and can be applied to other problems. And, it can be combined with multiple

heuristic algorithms to improve algorithm performance. The algorithm implements the steps as follows:

1) Ant pheromone distribution initialization, set number of iterations to 200;

2) According to the following transition probability, 30 ants are initialized in the vicinity and move. For each ant, define the objective function. In the basic ant colony algorithm model, the transition probability of the k-th ant from i location to j location is as follows:

$$p^{k}{}_{ij}(t)=\begin{cases}\dfrac{\left[\tau_j(t)\right]^{a}\left[\eta_{ij}(t)\right]^{\beta}}{\sum_{k\in k(t)}\left[\tau_{ij}(t)\right]^{a}\left[\eta_{ij}(t)\right]^{\beta}} & j\in k(t)\\ 0 & j\notin k(t)\end{cases} \tag{10}$$

where a is the pheromone concentration heuristic factor. The larger it's value, the more ants tend to choose the path that most ants take, $a=1.2$; β is the expected heuristic factor, which is the basis for ants to choose the next position. The larger it's value, the more ant tends to choose the path to the end point, $\beta=1.2$; $k(t)=\{1,2,...,n\}-u_k$ is the node that ant k is allowed to choose next; $\eta_{ij}=1/d_{ij}$ is the desired heuristic function, which represents the reciprocal of the distance d_{ij} between the positions i、j.

3) The objective function value of each ant is calculated, and the optimal path length of the current ant group is recorded;

4) Ants leave pheromone on the path they pass. The pheromones volatilize over time. According to the pheromone update equation, the strength of the pheromone is corrected. The pheromone update rule equation is as follows:

$$\tau_j(t+n)=(1-\rho)\tau_{ij}(t)+\Delta\tau_{ij}\quad \Delta\tau_{ij}=\begin{cases}\dfrac{Q}{L_k} & (i,j)\in p^{k}{}_{ij}\\ 0 & (i,j)\notin p^{k}{}_{ij}\end{cases} \tag{11}$$

Where ρ is the pheromone volatilization coefficient, $\rho\in(0,1)$, and $\rho=0.3$; $\Delta\tau_{ij}$ is the pheromone left by ant at the i、j position from t to $t+n$; Q is the pheromone intensity, and $Q=1$; L_k is the path length of ant k in this loop; $p^{k}{}_{ij}$ is the path taken by ant k from the start point to the end point in this loop.

5) Number of iterations plus 1, that is, $N=N+1$;

6) If the number of iterations does not reach 200, then return to the second step, otherwise the loop terminates and outputs the optimal heading/speed solution.

Under the constraints of collision avoidance, the path is planned through an improved artificial potential field algorithm. According to the above evaluation model, the evaluation value of each planning path is calculated to provide a search direction for ant colony algorithm, to improve the convergence speed, and to reduce the search time and complexity [27-29]. According to the evaluation value of collision avoidance, the optimal route is searched by heuristic ant colony algorithm. Finally, the USV's optimal heading and speed can be calculated.

4. Test Analysis

4.1 Simulation Results.

In the collision avoidance simulation program for USV, a disturbance model needs to be established to simulate the wind wave interference effect. Wang et al used white Gaussian noise and second-order transfer functions to simulate wind and wave disturbances in harsh sea conditions and used constant values to simulate the disturbance of ocean environment [23]. The USV's model and the model of steering gear established in this work under wind and wave interference is as follows:

$$y(s)=K_c w(s)\frac{K_\omega s}{s^2+2\zeta\omega_0 s+\omega_0{}^2},\begin{cases}y_{usv}(s)=\dfrac{2.1285s}{s^2+0.3636s+0.3672}\\ h_{duoji}(s)=\dfrac{0.05}{s+1}\end{cases} \tag{12}$$

Where $w(s)$ is white Gaussian noise, it's average value is zero, and it's power spectral density is 0.1; $K_c=5$ is a constant interference coefficient; $\zeta=0.3$ is a damping coefficient; $\omega_0=4.85/T_w$ is a dominant wave frequency; $K_\omega=2\xi\omega_0\sigma_m$ is a gain constant; $\sigma_m=\sqrt{0.0185T_w h_{1/3}}$ is a wave intensity coefficient; When $T_w=8s$ 、 $h_{1/3}=1.21m$, the interference coefficient is calculated as $\omega_0=0.6063$, $\sigma_m=0.4232$, and $K_\omega=0.1539$. At this time, the wind and wave interference is level 3 sea condition.

The starting point of USV is the lower left corner of the figure, and the end point is the upper right corner. Obstacles are red dots, its number is 18. Half of them are fixed obstacles and half are random obstacles. The blue curve is the collision avoidance trajectory of USV from starting point to end point. When using the traditional method and the improved algorithm, the USV's simulation track of collision avoidance of multiple static obstacles under the condition of wind and wave interference is shown in Fig. 5.

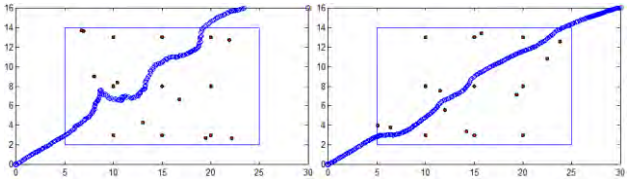

Fig. 5 Collision avoidance simulation trace of USV when using traditional algorithm (left) and the improved algorithm (right)

It can be seen from Fig 5 when using the traditional artificial potential field method, the problem of path jitter, oscillation occurs and frequent steering in the USV's collision avoidance process. When using the improved collision avoidance algorithm, it can solve the problems of path oscillating and jitter. USV's steering frequency is also reduced accordingly, and the collision avoidance path is relatively smooth, which enhances the stability under wind and wave interference.

It can be seen from the simulation results that the smaller control parameter n, the stronger oscillation. At this time, the function converges slowly and it is easy to overshoot; When n is larger, the prediction trend is increased, and the function converges faster; When the control parameter is increased from $n=5$ to $n=15$, it can be seen that the collision avoidance trajectory is smoother than before, and the potential field converges faster. At this time, the effect of collision avoidance experiment is most obvious. However, if n continues to increase, the slope of the potential field function is larger. And, the repulsion radius will become too short. At this time, the USV may not be able to turn the steering in time, which easily lead to hitting the obstacle.

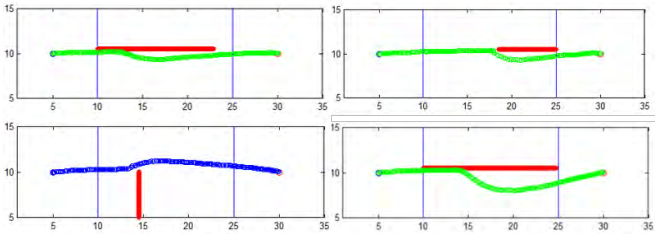

Fig. 6 USV's collision avoidance trajectory of the dynamic vessel mode: in front encounter mode, cross encounter mode and chase mode

Furthermore, experiment simulations of dynamic ship collision avoidance are performed. This experiment is divided into three modes: encounter mode, chase mode, and cross encounter. The red curve is the trajectory of dynamic obstacle vessel, and the green and blue curves are the trajectories of USV's collision avoidance. The USV's collision avoidance trajectory of the dynamic vessel mode is shown in Fig. 6.

The simulation experiments results show that the improved collision avoidance algorithm has the characteristics of high control precision, good robustness, and strong anti-interference. Compared

with the traditional artificial potential field algorithm, this algorithm's oscillation amplitude is small, the steering frequency is small, the potential field convergence speed is fast, and the ability of trend prediction is strong. The stability of the algorithm becomes stronger with environmental interference.

4.2 Experimental Results.

The improved collision avoidance algorithm was applied to the USV's real ship experiment in Taihu, Wuxi, and Tang Xunhu, Wuhan. The experiment's time was November 21, 2017. According to the meteorological data of the local Maritime Safety Administration, it is known that the weather is fine, the wind direction is southeast, the wind speed is level 2, the wave height is 0.42 meters. The zigzag experimental result is shown in Table 3.

Table 3 The zigzag experimental data of usv

Time/s	Rudder angle/◦& Heading angle/◦	Remark
1’82	15	15
5’82	15	28.2
9’44	-15	0
12’68	-15	-15
15’62	15	-24.7
23’06	15	15
26’56	-15	28.2

According to the calculation method in the literature [17], and the Z-type test data in Taihu Lake, the K,T parameters of the USV are obtained as follows:

$$K = 2.9097, T = 55.8855$$

Marine navigation radar and photoelectric camera are used to recognize targets obstacle's information such as distance, direction, and size. The static buoy is placed between the tracking points. Due to the corner reflector is mounted on the buoy, the navigation radar can easily recognize obstacle information. The longitude and latitude coordinates of the target point and the obstacles are shown in Table 4.

Table 4 Coordinate of the target points and obstacles

Num	Target point		Obstacle	
	longitude	latitude	longitude	latitude
1	120° 08' 03.7"E	31° 26' 31.4"N	120° 08' 05.7"E	31° 26' 29.6"N
2	120° 08' 07.7"E	31° 26' 27.9"N	120° 08' 07.1"E	31° 26' 25.5"N
3	120° 08' 06.5"E	31° 26' 23.1"N	120° 08' 04.4"E	31° 26' 22.0"N
4	120° 08' 02.3"E	31° 26' 21.0"N	120° 07' 59.8"E	31° 26' 22.6"N
5	120° 07' 57.4"E	31° 26' 24.3"N	120° 07' 58.2"E	31° 26' 26.8"N
6	120° 07' 59.0"E	31° 26' 29.4"N	120° 08' 01.4"E	31° 26' 30.8"N

During the collision avoidance experiment, the USV's speed was 12kn. In the figure, the purple point is the target tracking point, the red point is the static obstacle. And, the direction and distance information of the tracking point and obstacle is also indicated. The red line is the planned track and the blue is the actual track of USV. The navigation path and the collision avoidance trajectory of USV are transmitted back to the shore base on GPS's position information and displayed on monitoring software interface. The trajectory of collision avoidance using the traditional method and the improved collision avoidance algorithm is shown in Fig. 7-8.

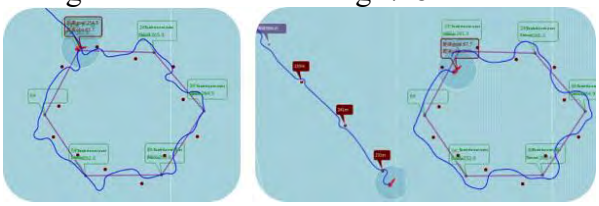

Fig. 7 Obstacles avoidance trace of USV when using traditional artificial potential field algorithm (left) and using the improved algorithm in Taihu Lake (right)

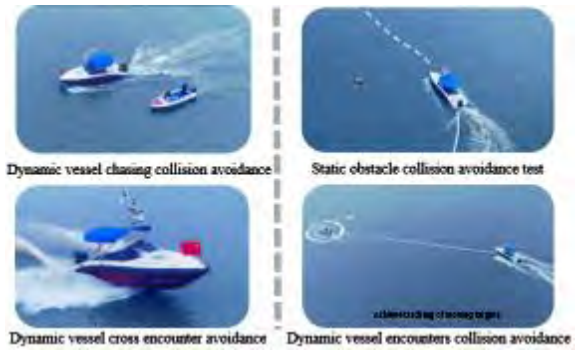

Fig. 8 Static obstacles and dynamic vessel collision avoidance test of USV when using the improved algorithm in Tang Xunhu Lake

It can be seen from Fig. 7-8, the traditional artificial potential field method has poor anti-interference and poor tracking capability characteristics in the wind and wave environment. There is a problem of frequent steering and the steering angle is excessively large during the collision avoidance process. The problem of frequency steering is solved by the improved collision avoidance algorithm. The collision avoidance trajectory is relatively smooth and the potential field converges faster. The anti-interference and stability of USV are enhanced. And, the algorithm has good tracking capability. The results of collision avoidance experiment are shown in Table 5-6.

Table 5 Results of experiments using traditional artificial potential field algorithms

Nun	Number of obstacles	Average collision avoidance time	Average number of steering	Shortest distance from obstacle	Shortest distance from the target point	Average steering angle
1	4	21s	25	19m	5m	30°
2	5	26s	26	25m	7m	35°
3	4	25s	23	23m	6m	34°
4	3	22s	20	20m	6m	28°
5	4	24s	22	22m	7m	32°

Table 6 Test results using the improved collision avoidance algorithm in this paper

Nun	Number of obstacles	Average collision avoidance time	Average number of steering	Shortest distance from obstacle	Shortest distance from the target point	Average steering angle
1	4	14s	12	14m	3m	18°
2	5	19s	15	19m	5m	23°
3	4	16s	13	18m	5m	20°
4	3	15s	10	15m	4m	18°
5	4	17s	12	17m	4m	19°

It can be seen from the above chart when using the collision avoidance algorithm of this work in the level 3 sea condition. The average collision avoidance time is 16.25 seconds, the average number of steering operations is 14 times, the average shortest distance to obstacles is 16.75m, the shortest distance to the target point is 4.25m, and the average corner angle of the rudder angle is 20 degrees.

From the results of lake experiment, it can be known that the collision avoidance algorithm fully satisfies the maneuverability of USV. And, it improves the problem of frequent steering and overshoot, and solves the problem that the traditional artificial potential field method is easy to fall into local minima and the target is unreachable. This algorithm has good tracking capability, strong anti-interference and high feasibility.

5. Conclusion

An improved collision avoidance algorithm based on artificial potential field algorithm and ant colony algorithm is designed by this work, to solve the problem of frequent steering of USV during collision avoidance in harsh sea condition. The results of simulation and experiment demonstrate: the improved collision avoidance algorithm has good robustness, anti-jamming and re-navigation and so on. Under complex sea conditions, this algorithm improves the problem of frequent steering and overshoot of USV, and solves the problem of traditional artificial potential field method that easily falls into local minimum points, and the problem of targets unreachable. Furthermore, the algorithm combines with USV's model and collision avoidance constraint conditions, and the evaluation model is established by this conditions. Through the evaluation function, the optimal path that fully meets the maneuverability requirements of USV is searched by the ant colony algorithm. Finally, the feasibility of the collision avoidance algorithm is verified by the results of the real ship experiment.

In this work, there are still problems in how to establish the USV's collision avoidance model in harsh sea state and large disturbance environment. The collision avoidance algorithm has poor adaptability under different sea conditions and environmental disturbances. The next step is to adopt an intelligent collision avoidance algorithm based on deep learning to solve this problem. It is necessary to improve the adaptability of the algorithm in different environments through the training sample of collision avoidance model, so that, to meet the USV maneuverability requirements under sea conditions of different levels. The problem of algorithm adaptability can be effectively improved by the neural network algorithm base on deep learning. Based on expert steering data (including sea experiment of a real ship, historical experience), accident case bases, and maritime rules, a collision avoidance training sample database of USV is established. And, an intelligent collision avoidance model based on deep learning is established. At the same time, it is necessary to establish an evaluation network model related to DCPA, TCPA, sailing time, path smoothness, path safety, and other collision avoidance performance indicators. Finally, the optimal heading and speed of USV are searched by the heuristic multi-objective Monte-Carlo algorithm, to implement the function of intelligent collision avoidance.

References

[1]. H. Ashrafiuon, K. R. Muske, L. C. McNinch, and R. A. Soltan, Sliding-mode tracking control of surface vessels, IEEE. T. Ind. Electron, vol. 55, no. 11, 2008, pp. 4004-4012.

[2]. J. Li, T. Li, and Y. Li, “NN-based adaptive dynamic surface control for a class of nonlinear systems with input saturation,” In: Proceedings of the 7th IEEE Conference on Industrial Electronics and Applications(ICIEA '12). Singapore, pp. 570-575, July 2012.

[3]. A. Sabanovic, Variable structure systems with sliding modes in motion control-a survey, IEEE. T. Ind. Inform, vol. 7, no. 2, 2011, pp. 212-223.

[4]. E. Lefeber, K. Y. Pettersen, and H. Nijmeijer, Tracking control of an underactuated ship, IEEE. T. Contr. Syst. T, vol. 11, no. 1, 2003, pp. 52-61.

[5]. M. Dunbabin, and A. Grinham, Quantifying spatiotemporal greenhouse gas emissions using autonomous surface vehicles, J. Field. Robot, vol. 34, no. 1, 2017, pp. 151-169.

[6]. Y. Valeriano-Medina, A. Martinez, L. Hernandez, H. Sahli, Y. Rodriguez, and J. R. Canizares, Dynamic model for an autonomous underwater vehicle based on experimental data, Math. Comp. Model. Dyn, vol. 19, no. 2, 2013, pp. 175-200.

[7]. P. H. Heins, B. L. Jones, and D. J. Taunton, Design and validation of an unmanned surface vehicle simulation model, Appl. Math. Model, vol. 48, no. 12, 2017, pp. 122-127.

[8]. J. Colito, Autonomous Mission Planning and Execution for Unmanned Surface Vehicles in Compliance with the Marine Rules of the Road, Master thesis, University of Washington, 2007.

[9]. Q. Luo, H. Zhang, and H. Wang, Application of improved artificial potential field approach in local path planning for mobile robot, Comp. Eng. Des, vol. 32, no. 4, 2011, pp. 1411-1413.

[10]. Y. Yang, and C. Wang, Obstacle Avoidance Method for Mobile Robots Based on Improved Artificial Potential Field Method and Its Implementation on MATLAB, J. U. Shanghai. Sci. T, vol. 35, no. 5, 2013, pp. 496-500.

[11]. F. XU, Research on Robot Obstacle Avoidance and Path Planning Based on Improved Artificial Potential Field Method, Com. Sci, vol. 43, no. 12, 2016, pp. 293-296.

[12]. G. Yin, Research on path planning of mobile robot based on improved artificial potential field, Tianjin University of Technology, 2017.

[13]. W. You, Z. Zhang, and W. Huang, Obstacle avoidance method research for robot based on fuzzy improved artificial potential field, Transducer. Microsyst T, vol. 35, no. 1, 2016, pp. 14-18.

[14]. H. Zhai, and J. Wang, Dynamic path planning research for mobile robot based on artificial potential field, J. Chongqing. U. Posts. Telecommun, vol. 27, no. 6, 2015, pp. 814-818.

[15]. J. Song, Obstacle Avoidance Problem Study of Robot Based on Artificial Potential Field Method, Shenyang University of Technology, 2014.

[16]. D. Zhao, X. Liu, and H. Zhou, Design of unmanned surface vehicle heading Controller Based on Fuzzy Neural Network, J. Central. China. Normal. U, vol. 52, no. 3, 2017, pp. 329-332.

[17]. W. Zheng, and C. Xiao, The parameter identification of KT equations on ship maneuverability, Ship. Sci. T, vol. 39, no. 17, 2017, pp. 129-132.

[18]. B. Hong, and L. Yang, Ship Handling, Dalian Maritime University Press, 2012.

[19]. .X. Lu, D. Yao, and B. Wang, Trimaran maneuverability prediction and its feature analysis, J. Naval. U. Eng, vol. 21, no. 1, 2009, pp. 47-53.

[20]. Z. Wang, The Research on Automatic Collision Avoidance for Unmanned Surface Vessel, Dalian Maritime University, 2013.

[21]. Y. Zhu, Research of Improved Ant Colony Algorithm and Its Application, Zhejiang University of Technology, 2010.

[22]. M. Shang, Z. Zhu, and T. Zhou, Research on Intelligent Anti-collision Method of USV Based on Improved Ant Colony Algorithm, Ship. Eng, vol. 16, no. 9, 2016, pp. 6-9.

[23]. Y.Wang, Based on Auto Disturbances Rejection Control algorithm for heading autopilot of Unmanned Surface Vessel design, Dalian Maritime University, 2014.

[24]. K. Liu, The Path Planning of Unmanned Surface Vehicle Based on Artificial Potenial Field and Ant Colony Algorithm, Hainan University, 2016.

[25]. B. Wu, Y. Xiong, and Y. Wen, Automatic collision avoidance algorithm for unmanned surface vessel based on velocity obstacles, J. Dalian. Marit. U, vol. 40, no. 2, 2014, pp. 13-16.

[26]. Y. Lu, Research on Path Planning Algoritms of Unmanned Surface Vehicle, Harbin Engineering University, 2010.

[27]. X. Zhuang, and L. Qi, Research on a Method for High Speed Unmanned Ship to Avoid Collision with Moving Obstacles, Ship. Electron. Eng, vol. 28, no. 12, 2008, pp. 100-102+122.

[28]. J. Liu, Research on Unmanned Surface Vessel collision avoidance system Based on Evolutionary genetic algorithm, Dalian Maritime University, 2015.

[29]. J. Zheng, J. Wu, and Y. Ma, A Hybrid optimization algorithm of Simulated Annealing and Particle Swarm for Unmanned Surface Vessel Path Planning, J. Ocean. U. China, vol. 46, no. 9, 2016, pp. 116-122.

[30]. P. Ren, A study on ship cllision avoidance-making based on cllision risk index, Dalian Maritime University, 2015.

[31]. D. Zhang, and F. Liu, Research and development trend of path planning base on artificial potential field method, Comput. Eng. Sci, vol. 35, no. 6, 2013, pp. 88-95.

[32]. B. Wu, Y. Wen, and B. Wu, Review and Expectation on Collision Avoidance Method of Unmanned Surface Vessel, J. Wuhan. U. T, vol. 40, no. 3, 2016, pp. 456-461.

[33]. Z. Piao, and C. Guo, Maneuvering mathematical model and course control of POD-driven ship. In: Proceedings of the 6th International Conference on Information Science and Technology (ICIST '16). Dalian, China, pp. 301–305, May 2016.

[34]. M. Caccia, G. Bruzzone, and R. Bono, A practical approach to modeling and identification of small autonomous surface craft, IEEE. J. Oceanic. Eng, vol. 33, no. 2, 2008, pp. 133-145.

[35]. M. Chen, S. S.Ge, and B. V. E. How, Robust adaptive neural network control for a class of uncertain MIMO nonlinear systems with input nonlinearities, IEEE. T. Neural. Networ, vol. 21, no. 5, 2010, pp. 796-812.